

# Selection for mutational robustness in finite populations

Robert Forster<sup>a</sup>, Christoph Adami<sup>a,b</sup>, Claus O. Wilke<sup>c,\*</sup>

<sup>a</sup>Digital Life Laboratory, California Institute of Technology, Pasadena, CA 91125, USA

<sup>b</sup>Keck Graduate Institute of Applied Life Sciences, 535 Watson Drive, Claremont, CA 91711, USA

<sup>c</sup>Section of Integrative Biology and Center for Computational Biology and Bioinformatics, University of Texas at Austin, Austin, TX 78712, USA

Received 1 September 2005; received in revised form 7 June 2006; accepted 23 June 2006

Available online 30 June 2006

## Abstract

We investigate the evolutionary dynamics of a finite population of RNA sequences replicating on a neutral network. Despite the lack of differential fitness between viable sequences, we observe typical properties of adaptive evolution, such as increase of mean fitness over time and punctuated-equilibrium transitions, *after* initial mutation–selection balance has been reached. We find that a product of population size and mutation rate of approximately 30 or larger is sufficient to generate selection pressure for mutational robustness, even if the population size is orders of magnitude smaller than the neutral network on which the population resides. Our results show that quasispecies effects and neutral drift can occur concurrently, and that the relative importance of each is determined by the product of population size and mutation rate.

© 2006 Elsevier Ltd. All rights reserved.

**Keywords:** RNA secondary structure folding; Quasispecies; Neutral networks; Mutational robustness

## 1. Introduction

The quasispecies model of molecular evolution (Eigen, 1971; Eigen and Schuster, 1979) predicts that selection acts on clouds of mutants, the *quasispecies*, rather than on individual sequences, if the mutation rate is sufficiently high. RNA viruses tend to have fairly high mutation rates (Drake, 1993; Drake and Holland, 1999), and therefore the quasispecies model is frequently used to describe the evolutionary dynamics of RNA virus populations (Domingo, 1992, 2002; Domingo and Holland, 1997; Domingo et al., 2001). However, this use has generated criticism (Holmes and Moya, 2002; Jenkins et al., 2001), because quasispecies theory, as it was originally developed, assumes an infinite population size and predicts deterministic dynamics. Viral populations, on the other hand, are finite and subject to stochastic dynamics and neutral drift.

However, the hallmark of quasispecies dynamics—the existence of a mutationally coupled population that is the target of selection in its entirety—does not presuppose an

infinite population size or the absence of neutral drift (Demetrius et al., 1985; Nowak and Schuster, 1989; van Nimwegen et al., 1999; Wilke, 2004). Rather, infinite populations were used by Eigen (1971) and Eigen and Schuster (1979) to simplify the mathematics of the equations describing the population dynamics. Even though technically, the quasispecies solution of Eigen and Schuster, defined as the largest eigenvector of a suitable matrix of transition probabilities, exists only for infinite populations after an infinitely long equilibration period, it would be wrong to conclude that the cooperative population structure induced by mutational coupling disappears when the population is finite. We show here that quasispecies dynamics are evident in fairly small populations (effective population size  $N_e \leq 1000$ ), and that these dynamics cross over to pure neutral drift in a continuous manner as the population size decreases.

We simulate finite populations of self-replicating RNA sequences and look for an unequivocal marker for quasispecies dynamics in this system, the selection of mutational robustness (van Nimwegen et al., 1999; Bornberg-Bauer and Chan, 1999; Wilke, 2001a; Wilke and Adami, 2003). We choose RNA secondary structure

\*Corresponding author. Tel.: +1 512 471 6028.

E-mail address: [cwilke@mail.utexas.edu](mailto:cwilke@mail.utexas.edu) (C.O. Wilke).

folding (Hofacker et al., 1994) as a fitness determinant because it is a well-understood model in which the mapping from sequence to phenotype is not trivial. The non-triviality of this mapping is crucial for the formation of a quasispecies, as we will explain in more detail later.

Since the existing literature on the evolution of RNA secondary structures is extensive, we will now briefly review previous works and then describe how our study differs. We can subdivide the existing literature broadly into three categories: (i) studies that investigate how secondary structures are distributed in sequence space; (ii) studies that investigate how sequences can evolve from one structure into another; and (iii) studies that investigate the evolution of sequences that all fold into the same secondary structure, that is, the evolution of sequences on a single neutral network.

Studies in the first category have established the importance of neutral networks for RNA secondary structure folding (Schuster et al., 1994; Reidys et al., 1997). All sequences folding into the same secondary structure form a network in genotype space, that is, a graph that results from including all these sequences as vertices, and including an edge between two such vertices if a single mutation can interconvert the two sequences. The number of edges connected to a vertex is called the degree of neutrality of that vertex (i.e. sequence). These neutral networks span large areas of sequence space, the neutral networks' size distribution follows a power law, and for any two secondary structures of comparable size, there are areas in sequence space in which sequences folding into both structures can be found in close proximity (Schuster et al., 1994; Grüner et al., 1996a, b; Reidys et al., 1997). Further, the fitness landscapes derived from RNA secondary structure folding are similar to basic models of fitness landscapes, but differ in details (Fontana et al., 1993; Cowperthwaite et al., 2005), and are highly epistatic (Wilke and Adami, 2001; Wilke et al., 2003).

In the second category of studies, the main result of investigating the evolution of secondary structures is that evolution proceeds in a stepwise fashion: a single secondary structure dominates the population for an extended period of time (an epoch), but intermittently a new, improved structure will appear and take over the population (Huynen et al., 1996; Fontana and Schuster, 1998a, b). During the epochs when the population is seemingly static, the population diffuses over the neutral network of the currently dominant structure. It is primarily because of this prolonged diffusion that the population has a chance to discover a new structure with higher fitness (Huynen, 1996; Huynen et al., 1996; Fontana and Schuster, 1998a, b). Details of the diffusion process and the transition probabilities from one structure to another have been worked out (Forst et al., 1995; Huynen et al., 1996, see also next paragraph).

We can interpret studies in the third category as describing the evolutionary dynamics during the epochs of phenotypic stasis observed in the evolution of secondary

structures. As already mentioned, the sequences diffuse over the neutral network, and any specific sequence is rapidly lost from the population (Huynen et al., 1996; Reidys et al., 2001). However, the sequences do not diffuse as a single, coherent unit, but instead form separate clusters that diffuse independently from each other (Forst et al., 1995; Huynen et al., 1996). It is useful to extend Eigen's concept of the error threshold (Eigen, 1971) to distinguish between the genotypic error threshold, that is, the mutation rate at which a specific sequence cannot be maintained in the population, and the phenotypic error threshold, that is, the mutation rate at which a given secondary structure cannot be maintained in the population (Forst et al., 1995; Reidys et al., 2001). For RNA, the genotypic error threshold occurs usually for an infinitesimally small positive mutation rate, while the phenotypic error threshold occurs at fairly large mutation rates (Forst et al., 1995; Reidys et al., 2001). The exact position of the phenotypic error threshold depends on the size of the neutral network and the fitness of suboptimal secondary structures (Reidys et al., 2001).

It is important to distinguish the diffusion over a neutral network from drift in a completely neutral fitness landscape (Derrida and Peliti, 1991; Higgs and Derrida, 1991, 1992). If the product of population size and mutation rate is sufficiently high, then on a neutral network (where a fraction of all possible mutations is deleterious) there is a selective pressure that keeps the population away from the fringes of the neutral network, and pushes it towards the more densely connected areas in the center of the neutral network (van Nimwegen et al., 1999; Bornberg-Bauer and Chan, 1999; Wilke, 2001a). This selective pressure has been termed "selection for mutational robustness" (van Nimwegen et al., 1999), and is a tell-tale sign that selection occurs in the quasispecies mode on clouds of mutants, rather than on individual sequences. Van Nimwegen et al. and Bornberg-Bauer and Chan were the first to develop a formal theory for this effect, but anecdotal evidence for it had already been observed previously (Huynen and Hogeweg, 1994; Forst et al., 1995). The theory developed by van Nimwegen et al. and Bornberg-Bauer and Chan applies only to infinite populations. Nevertheless, simulations have shown that this effect occurs also in large but finite populations if the mutation rate is sufficiently large (van Nimwegen et al., 1999; Wilke, 2004).

According to the quasispecies model, mutational robustness is as important a component of fitness as is replication speed (Schuster and Swetina, 1988; Wilke et al., 2001; Wilke, 2001b). This observation suggests that a sudden transition to increased mean fitness may not only be caused by the discovery of a sequence with higher replication rate, but also by the discovery of a more densely connected region of the neutral network the population is already residing on, without any obvious change in the sequences' phenotype (Wilke, 2001a). Here, we study these types of transitions, which change the population mean fitness while the secondary structure remains unchanged, and which

occur *after* initial mutation–selection balance has been reached.

In our simulations, we consider all RNA sequences that fold into a specific target secondary structure as viable. All viable sequences have the same fitness, arbitrarily set to one. All RNA sequences that do not fold into the target secondary structure are non-viable, with fitness 0. There is no phenotypic error threshold in our simulations, and the target structure can only be lost from the population through sampling noise. The latter outcome is extremely unlikely for all but the smallest population sizes. However, if it occurs the population dies, because all remaining sequences have fitness zero. Our choice of fitness landscape guarantees that all changes that we see in mean fitness must be caused by changes in the population neutrality. (Here and in the following, we refer to the average degree of neutrality among viable members of the population as the population neutrality or simply the *neutrality*.)

## 2. Materials and methods

We consider a population of fixed size  $N$  composed of asexual replicators whose probability of reproduction in each generation is proportional to their fitness (Wright–Fisher sampling). The members of the population are RNA sequences of length  $L = 75$ , and their fitness  $w$  is solely a function of their secondary structure. Those that fold into a specific target secondary structure are deemed viable with fitness  $w = 1$ , while those that fold into any other shape are non-viable ( $w = 0$ ). The average fitness  $\langle w \rangle$  of the population is therefore the fraction of living members out of the total population. RNA sequences are folded into the minimum free energy structure using the Vienna Package (Hofacker et al., 1994), and dangling ends are given zero free energy (Walter et al., 1994). For a given simulation, an initial RNA sequence is selected uniformly at random and its minimum-energy secondary structure defines the target structure for this simulation, thereby determining a neutral network on which the population evolves for a time of  $T = 50,000$  generations. Mutations occur during reproduction with a fixed probability  $\mu$  per site, corresponding to an average genomic mutation rate  $U = \mu L$ .

Our simulations spanned a range of genomic mutation rates and population sizes, and we performed 50 independent replicates for each of the pairs  $(U, N)$ , starting each with a different randomly chosen initial sequence. To study mutation rate effects, we considered a fixed population size of  $N = 1000$ , across a range of genomic mutation rates, using  $U = 0.1, 0.3, 0.5, 1.0$ , and  $3.0$ . To study effects due to finite population size, we considered a fixed mutation rate of  $U = 1.0$ , using population sizes of  $N = 30, 100, 300$ , and  $1000$ .

The degree of neutrality of a sequence was determined by calculating the fraction of mutations that did not change the minimum-energy secondary structure. Thus, if  $N_v$  of all  $3L$  one-point mutants of a sequence retain their structure, the degree of neutrality of that sequence is given by

$v = N_v/3L$ . Because sequences that do not fold into the target structure have zero fitness, a sequence's degree of neutrality is equal to the mean fitness of all possible single mutants. We recorded the population's average fitness every generation, while the population's average neutrality, being much more computationally expensive, was calculated only at the start and end of each replicate. For illustrative purposes, select replicates of interest were recreated using the original random seed, and the population neutrality was recorded every 100 generations.

To observe the signature of natural selection acting within our system, we derived a statistical approach to identify transitions in the population's average fitness  $\langle w \rangle$ . If a beneficial mutation appears and is subsequently fixed in the population, we expect to observe a step increase in the population's average fitness. (Throughout this paper, by beneficial mutations we mean mutations that increase a sequence's degree of neutrality, and thus indirectly the mean fitness of the population. We emphasize again that such selective sweeps must be due to periodic selection of quasispecies for increased mutational robustness, since there are no mutations that increase the fitness of a viable sequence beyond the value 1 in our system.)

In light of the fluctuations in the population's average fitness due to mutations and finite population effects, we employed statistical methods to estimate the time at which the increase in average fitness occurred and associated a  $p$ -value with our level of confidence that a transition has occurred. Our approach can be thought of as a generalization of the test for differing means between two populations (those before and after the mutation), except that the time of the mutation's occurrence is unknown a priori. For a full derivation and discussion of our approach, see the Appendix. While our algorithm can be applied recursively to test for and identify multiple transitions that may occur in a single simulation, unless otherwise noted, we considered only the single most significant transition found.

## 3. Results

Because replicates were initialized with  $N$  (possibly mutated) offspring of the randomly chosen ancestor, the simulation runs did not start in mutation–selection balance. Typically, we observed an initial equilibration period of 50 to 200 generations, after which the population's fitness and neutrality stabilized, with fluctuations continuing with magnitude in proportion to the mutation rate. As predicted by van Nimwegen et al. (1999), during the equilibration period, we observed in most replicates beneficial mutations that increased the equilibrium level of both average fitness and neutrality. These mutations led to the initial formation of a quasispecies in a central region of the neutral network. For the remainder of this paper, we are not interested in this initial equilibration, but in transitions towards even more densely connected areas of the neutral network once the initial equilibration has occurred.

To determine if such a transition has occurred, we need a method to distinguish significant changes in the population's mean fitness from apparent transitions caused by statistical fluctuations. We devised a statistical test (see Appendix for details) that can identify such transitions and assign a  $p$ -value to each event. We found that transitions to higher average fitness occurred in over 80% of simulations across all mutation rates studied, if we considered all transitions with  $p$ -values of  $p < 0.05$ . Fig. 1 shows a particularly striking example of such a transition ( $p$ -value  $\leq 10^{-7}$ ), where a 5.0% increase in average fitness occurs at  $t = 9814$ . A similar analysis of the average population neutrality (not usually available, but computed every generation specifically in this case) finds an increase of 11.2% occurring at  $t = 9876$ , with the same level of confidence. The multiple transitions shown in the Fig. 1 are the results of recursively applying our step-finding algorithm until no steps are found with  $p < 0.05$ .

Depending on the mutation rate, a step size as little as 0.04% in the population's average fitness could be statistically resolved in a background of fitness fluctuations several times this size. For comparison, typical noise levels, as indicated by the ratio of the standard deviation of the fitness to its mean, ranged from 0.7% to 6.6% over the mutation rates studied. Note that fluctuations in the population's neutrality level are much smaller, due to the additional averaging involved. However, because neutrality is much more expensive computationally, and would also be difficult to measure in experimental viral populations, we used mean fitness as an indicator of transitions throughout this paper.

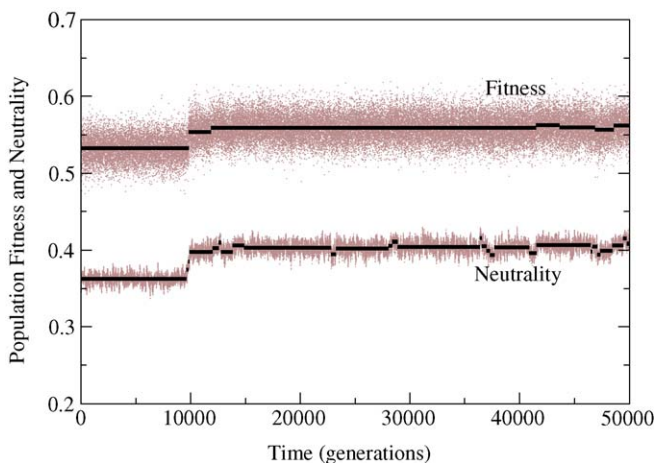


Fig. 1. Average fitness and neutrality of a population during a single simulation at a genomic mutation rate of  $U = 1.0$ . At  $t = 9814$ , a 5% increase in the population's average fitness occurs at the  $p < 10^{-7}$  level, with a corresponding transition in the population's average neutrality. Smaller transitions occur throughout the simulation run. The solid lines indicate the epochs of constant fitness and neutrality, as determined by our step-finding algorithm. As explained in the Appendix, the application of this algorithm to the neutrality data is for illustrative purposes only. Because of temporal autocorrelations in the neutrality, not all steps that the algorithm identifies are statistically significant.

Fig. 2 shows the average size of the most significant step observed as a function of the mutation rate. At low mutation rates, such as  $U = 0.1$ , the smaller observed step size corresponds to the fact that 90% of the population is reproducing without error, and hence improvements in neutrality can only increase the population's fitness in the small fraction of cases when a mutation occurs. At higher mutation rates the step sizes increase, reflecting the larger beneficial effect of increased neutrality under these conditions.

In about 10% of all simulations with statistically significant changes in fitness, the most significant change in fitness was actually a step *down*, that is, a fitness loss, rather than the increase in fitness typically observed. Negative steps in average fitness occur due to stochastic fixation of detrimental mutations at small population sizes (Kimura, 1962). These negative fitness steps, however, are generally much smaller than the typical positive step size. The average size of these negative steps was between 0.09 and 0.77%, compared with an average positive step size between 0.27% and 2.33% (see Fig. 3).

We specifically studied the role of finite population size and its effects on neutral drift by considering populations of size  $N = 30, 100, 300$ , and 1000 at a constant genomic mutation rate of  $U = 1.0$ . We again performed 50 replicates at each population size, and the distribution of statistically significant step sizes are shown in Figs. 4 (biggest step only) and 5 (all steps). While the larger population's distributions show a clear bias towards positive steps in fitness, the distributions become increasingly symmetric about zero for smaller population sizes. A gap around zero fitness change becomes increasingly pronounced in smaller populations, as the fluctuations in fitness due to finite population size preclude us from statistically distinguishing small step sizes from the null hypothesis that no step has occurred.

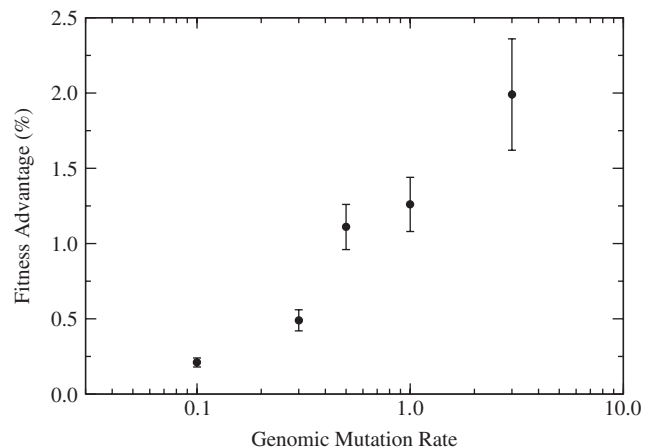


Fig. 2. Average step size as a function of genomic mutation rate ( $U = 0.1, 0.3, 0.5, 1.0, 3.0$ ). Step size is measured by percent increase in the population's fitness, with only runs significant at the  $p < 0.05$  level shown. Error bars are standard error.

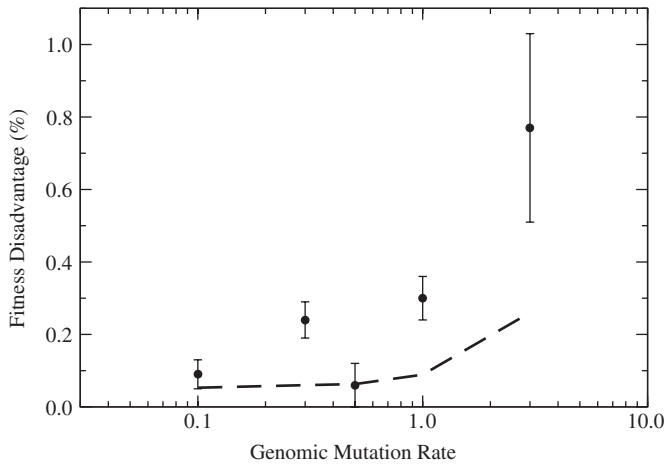


Fig. 3. Average step size  $|s|$  of statistically significant drops in fitness (at the  $p < 0.05$  level). Step size is measured by relative decrease in population fitness, and error bars are standard error. The dotted line indicates  $2|s| = 1/N_e$ , a selective disadvantage consistent with neutral drift in a finite population.  $N_e$  is the average number of living members of the population (effective population size).

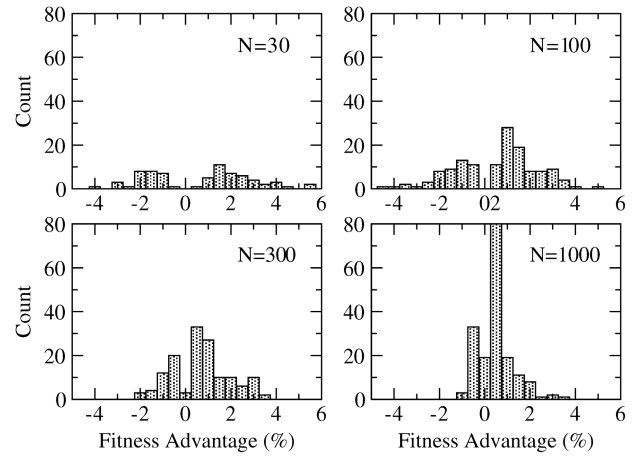


Fig. 5. Distribution of sizes of all significant steps (at  $p < 0.05$ ) in each run, out of 50 runs at four population sizes ( $U = 1$ ). While these distributions are more symmetrical than those of Fig. 4, a substantial skew towards positive step sizes is still evident for the larger population sizes.

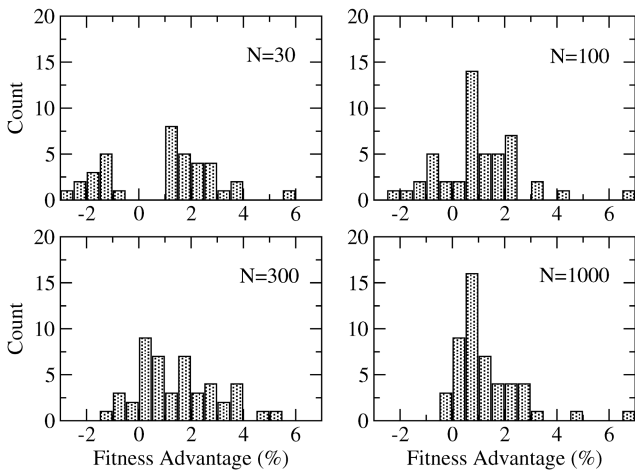


Fig. 4. Distribution of sizes of the most significant step (at  $p < 0.05$ ) in each run, out of 50 runs at four population sizes ( $U = 1$ ). At small population sizes, the distribution is almost symmetric about zero since most mutations are of less benefit than the  $1/N_e$  probability of fixation due to drift. At large sizes, selection is evident from the positively skewed distribution.

We also kept track of the consensus sequence in our simulations, to determine whether the population underwent drift while under selection for mutational robustness. In the runs with  $N = 1000$ , the consensus sequence accumulated on average one substitution every 2–3 generations. As such rapid change might be caused by sampling effects, we also studied the speed at which the consensus sequence changed over larger time windows. Using this method with window lengths of 50 and 100 generations, we found that the consensus sequence accumulated one substitution every 10–20 generations (window size 50 generations) or 15–30 generations (window

Time	Consensus Sequence
1000	CGACAGACAAGUAAUAAAAAAAAACUGCCAUGCAUUGCAAAAAGUGAAGCAUGCUAAACUAGUCUGCGAAAAAAA
2000	.....G.....A.....U.....A.....
3000	.....C.....A.....C.....
4000	.....A.....A.....C.....C.....C.....U.....
5000	.....U.....U.....A.....A.....A.....A.....C.....
6000	.....U.....U.....A.....C.....G.....A.....C.....C.....A.....
7000	.....AC.....C.....A.....A.....A.....
8000	.....A.....A.....U.....A.....C.....
9000	.....A.....C.....A.....U.....A.....A.....
10000	.....C.....A.....AU.....A.....A.....A.....U.....C.....
11000	.....U.....A.....A.....U.....A.....A.....A.....A.....
12000	.....U.....A.....A.....
13000	.....AA.....G.....G.....
14000	.....G.....U.....U.....
15000	.....A.....U.....A.....A.....
16000	.....G.....A.....U.....
17000	.....A.....A.....
18000	.....C.....G.....G.....U.....
19000	.....A.....A.....A.....A.....
20000	.....U.....U.....G.....G.....
21000	.....A.....A.....A.....A.....
22000	.....C.....AA.....A.....A.....
23000	.....A.....C.....C.....G.....G.....
24000	.....G.....C.....C.....G.....G.....
25000	.....U.....A.....A.....A.....A.....U.....U.....
	((((((((.....(((((.....))))))))).....)))))).....

Fig. 6. Change in the consensus sequence over time, from the same simulation run as presented in Fig. 1. Dots in the alignment indicate that the base at this position is unchanged from the previous line. The bottom row shows the target secondary structure in parentheses notation for reference.

size 100 generations). Thus, we find that the populations continue to drift rapidly throughout the simulation runs, and never settle down to a stable consensus sequence. Fig. 6 shows the evolution of the consensus sequence over time for the same simulation run as shown in Fig. 1.

Finally, to confirm that our finite population was not sampling the entire neutral network during our simulations, we estimated the size of typical neutral networks in our simulation. Previous works have shown that the

distribution of network sizes follows a power law (Zip's law) (Schuster et al., 1994; Grüner et al., 1996a). However, these studies are not directly applicable to our situation, because they looked at sequences of different lengths and/or coarse-grained secondary structures. Therefore, we generated a sample of  $10^7$  randomly chosen RNA sequences of length  $L = 75$ , determined the secondary structure of each sequence, and counted how often each distinct secondary structure appeared in the sample. We found that 0.00886% of all sequences had a minimum-energy conformation that was completely unfolded (contained not a single base pair). Among all other secondary structures, we found a power law decay of the frequency of the neutral networks with size (Fig. 7), which suggests a frequency distribution of sizes  $s$  given by  $F(s) \sim s^{-4}$ . On the basis of this power law, we can estimate the size of a typical neutral network found by random sampling. Assume that  $F(s) = C(1 + s/b)^{-4}$ , where  $C$  is a normalization constant and  $b$  determines the network size at which the distribution levels off (we discuss the limit  $b \rightarrow 0$  below). We can calculate  $C$  from

$$1 = \int_0^{\infty} F(s) ds = \frac{Cb}{3}, \quad (1)$$

and find  $C = 3/b$ . Likewise, we can calculate the average network size  $\langle s \rangle$ , and find

$$\langle s \rangle = \int_0^{\infty} sF(s) ds = \frac{b}{2}. \quad (2)$$

Now, we calculate the probability that a randomly chosen network is a factor  $x$  larger or smaller than  $\langle s \rangle$ . The probability that a randomly chosen sequence will belong to a network of size  $s$  is proportional to  $sF(s)$ . Thus, we calculate the probability to obtain a network at least a

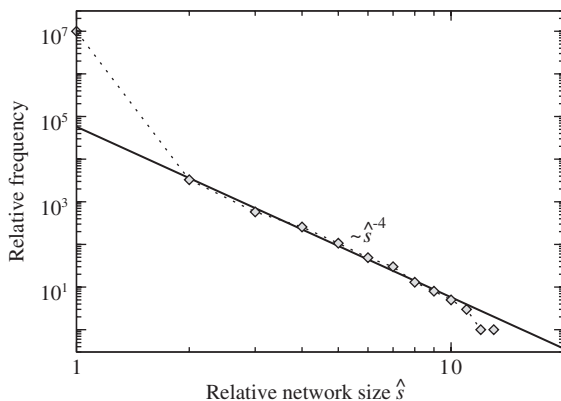


Fig. 7. Relative frequency of neutral networks generated by RNA sequences of length  $L = 75$ , in a sample of  $10^7$  randomly generated sequences. The relative network size  $\hat{s}$  corresponds to the number of times a given structure occurred in our sample. The tail is well approximated by a power law decay of the form  $\hat{s}^{-4}$  (solid line). Not shown is a single network of size 886, corresponding to a minimum-energy state that is completely unfolded. The deviation of the point corresponding to  $\hat{s} = 1$  from the power law behavior is expected because of the discreteness of the sample; this point subsumes the contributions from all networks too small to have their relative size accurately measured by our sample.

factor  $x$  smaller than  $\langle s \rangle$  as

$$P(s \leq \langle s \rangle / x) = \int_0^{\langle s \rangle / x} \frac{s}{\langle s \rangle} F(s) ds = \frac{6x + 1}{(2x + 1)^3}. \quad (3)$$

This probability decays as  $x^{-2}$ , which means we are extremely unlikely to randomly choose a network that is two or more orders of magnitude smaller than an average-size network. Similarly, we calculate the probability to obtain a network at least a factor  $x$  larger than  $\langle s \rangle$  as

$$P(s \geq x \langle s \rangle) = \int_{x \langle s \rangle}^{\infty} \frac{s}{\langle s \rangle} F(s) ds = \frac{12x + 8}{(x + 2)^3}. \quad (4)$$

This probability also decays as  $x^{-2}$ , which means we are also extremely unlikely to randomly chose a network that is two or more orders of magnitude larger than an average-size network. Thus, our analysis shows that the networks we typically encounter by folding randomly chosen RNA sequences are approximately of the size of the mean neutral network.

In the limit of  $b \rightarrow 0$ , we have a pure power law distribution,  $F(s) = C's^{-4}$ . In this case a similar calculation shows that there must be a minimum network size  $s_{\min}$ , and this network size is given by  $s_{\min} = \frac{2}{3}\langle s \rangle$ . Again, networks both significantly smaller or larger than  $\langle s \rangle$  are rare, and the typical network size is given by the average network size.

We now derive a lower bound on the average network size. We represent each RNA secondary structure in dot-and-parenthesis notation, where matched parentheses indicate a bond between the bases at those points in the sequence and dots represent unpaired bases. The number of valid strings of length  $L$  can be counted using Catalan numbers  $\text{Cat}(n) = \binom{2n}{n} / (n + 1)$ , which give the number of ways to open and close  $n$  pairs of parentheses (van Lint and Wilson, 2001). Since there are  $4^L$  possible RNA sequences, we obtain for the average network

$$\langle s \rangle = 4^L \left/ \sum_{i=0}^{\lfloor L/2 \rfloor} \text{Cat}(i) \binom{L}{L-2i} \right. \approx 1.1 \times 10^{12} \quad (5)$$

for  $L = 75$ . The above expression is a lower bound on the true average network size because the denominator includes some unphysical structures such as hairpins with fewer than three bases. Schuster et al. (1994) have shown that there are asymptotically  $S(L) = 1.4848L^{-3/2}(1.8488)^L$  planar RNA secondary structures of length  $L$ , where certain physically unlikely structures such as hairpins smaller than three bases and isolated base pairs are excluded (but note that not all of these excluded structures are necessarily impossible in our simulations). Using the expression  $S(L)$  in place of the denominator in Eq. (5) gives an alternative estimate for the average network size of  $6.0 \times 10^{27}$ , suggesting that real networks may be much larger on average than the lower bound we derive. In comparison, the number of possible distinct genotypes that can appear in each simulation is maximally  $NT = 5 \times 10^7$ , many orders of magnitude below the typical network size.

#### 4. Discussion

In the study of varying mutation rates, the observed increases in the population's fitness in almost all replicates demonstrate the action of natural selection. Since all viable sequences are neutral and hence enjoy no reproductive fitness advantage, this selection acts on increasing the population's robustness to mutations through increases in its average neutrality (as seen in Fig. 1). Thus, these results show evidence that a quasispecies is present in almost all cases, even though the difference between a randomly drifting swarm and a population structured as a quasispecies decreases as the population size and mutation rate decrease. Our results also show evidence of drift leading to the fixation of detrimental mutations in some populations. The negative steps observed (Fig. 3) were comparable in size to  $1/N_e$ , the probability of a neutral mutation drifting to fixation.

In the study of varying population sizes, the distribution of mutational effects on fitness showed an increasing bias towards beneficial rather than detrimental mutations as the population's size increased (Figs. 4 and 5). At population sizes 100, 300, and 1000, the clear positive bias of mutational effects illustrates the presence of a quasispecies, where natural selection is able to act to improve the population's neutrality and hence its robustness to mutations. As the fluctuations in fitness due to small population size become more significant, selection for neutrality becomes less relevant when the  $1/N_e$  sampling noise exceeds the typical step size of 1%. At the smallest population size of 30, there still seems to be a bias towards beneficial mutations, but the evidence is less clear and more replicates are probably necessary to observe a clear signal of quasispecies dynamics.

Our analysis of the size of neutral networks typically encountered by random sampling showed that the typical randomly chosen network has a size of the order of the average network size. Since the average network size (as given by the lower bound Eq. (5)) is many orders of magnitude larger than the number of sequences produced during a simulation run, we know that the system is non-ergodic and the population cannot possibly have explored the whole neutral network.

In our simulations, one of the hallmarks of quasispecies evolution—the periodic selection of more mutationally robust quasispecies on a neutral network—occurs at population sizes very significantly smaller than the size of the neutral network they inhabit. Despite small population sizes, if the mutation rate is sufficiently high (in the simulations reported here, it appears that  $NU \gtrsim 30$  is sufficient), stable frequency distributions significantly different from random develop on the partially occupied network in response to mutational pressure. Most importantly, we have shown that genetic drift can occur simultaneously with quasispecies selection, and becomes dominant as  $NU$  decreases. Thus, we find that both quasispecies dynamics and neutral drift occur at all finite population

sizes and mutation rates, but that their relative importance changes.

The existence of a stable consensus sequence in the presence of high sequence heterogeneity has long been used as an indicator of quasispecies dynamics (Domingo et al., 1978; Steinhauer et al., 1989; Eigen, 1996; Jenkins et al., 2001; Domingo, 2002). In contrast, the genotypic error threshold for evolution of RNA sequences typically occurs at any small positive mutation rate (Forst et al., 1995; Huynen et al., 1996; Reidys et al., 2001). Here we have shown that quasispecies dynamics can be present while the consensus sequence changes over time. In our simulations, the consensus sequence drifts randomly, in a manner uncorrelated with the transitions in average fitness that we detect. Thus, quasispecies dynamics does not require individual mutants to be stably represented in the population, nor does it require a stable consensus sequence.

The population structure on the neutral network is strongly influenced by the mutational coupling of the genotypes that constitute the quasispecies. This coupling arises because mutations are not independent in the landscape we studied. Rather, as in most complex fitness landscapes, single mutations at one locus can affect the fitness effect of mutations at another (a sign of epistasis, Wolf et al. (2000)). In the fitness landscape investigated here, mutations at neutral or non-neutral (i.e. lethal) sites can influence the degree of neutrality of the sequence. The absence of epistatic interactions between the neutral mutations in the fitness landscape studied by Jenkins et al. (2001) explains the absence of quasispecies dynamics in these simulations. Theoretical arguments show that a non-interacting neutral region in a genome does not alter the eigenvectors of the matrix of transition probabilities, and therefore cannot affect quasispecies dynamics.

Using fitness transitions on neutral networks as a tool to diagnose the presence of a quasispecies has a number of interesting consequences from a methodological point of view. Clearly, because selection for robustness is a sufficient criterion for quasispecies dynamics but not a necessary one, the absence of a transition does not imply the absence of a quasispecies. At the same time, as the population size decreases, fluctuations in fitness become more pronounced, rendering the detection of a transition more and more difficult. Theoretical and numerical arguments suggest that small populations at high mutation rate cannot maintain a quasispecies (van Nimwegen et al., 1999), so the disappearance of the mutational robustness signal at small population sizes is consistent with the disappearance of the quasispecies. However, the type of analysis carried out in this work does not lend itself to detecting quasispecies in real evolving RNA populations, because the fitness landscape there cannot be expected to be strictly neutral. Instead, transitions from one peak to another of different height (Burch and Chao, 2000; Novella, 2004) are likely to dominate. Quasispecies selection transitions such as the one depicted in Fig. 1

can, in principle, be distinguished from peak-shift transitions in that every sequence before and after the transition should have the same fitness. Unfortunately, pure neutrality transitions are likely to be rare among the adaptations that viruses undergo, and the data necessary to unambiguously identify them would be tedious if not impossible to obtain.

Our simulations provide evidence of selection for mutational robustness occurring through increasing the degree of neutrality of RNA sequences at population sizes far below the size of the neutral network that the sequences inhabit. Such increases in the degree of neutrality was recently found in a study that compared evolved RNA sequences to those deposited in an aptamer database (Meyers et al., 2004). For example, the comparison showed that human tRNA sequences were significantly more neutral, and hence more robust to mutations, than comparable random sequences that had not undergone evolutionary selection. However, we must caution that while in our simulations, selection for mutational robustness is the only force that can cause the sequences to become more mutationally robust, in real organisms other forces, for example selection for increased thermodynamic stability (Bloom et al., 2005), could have similar effects.

An experimental system that is quite similar to our simulations, probably more so than typical RNA viruses, is that of *viroids*—unencapsidated RNA sequences of only around 300 bases—capable of infecting plant hosts. Viroid evolution appears to be limited by the need to maintain certain secondary structural aspects (Keese and Symons, 1985), which is consistent with our fitness assumptions. Furthermore, in Potato spindle tuber viroid (PSTVd), a wide range of single and double mutants are observed to appear after a single passage (Owens and Thompson, 2005), suggesting that a quasispecies rapidly forms under natural conditions. Viroids may have agricultural applications as they are capable of inducing (desirable) dwarfism in certain plant species (Hutton et al., 2000), and as such, a better understanding of their evolutionary processes may help to direct future research efforts.

Making the case for or against quasispecies dynamics in realistic, evolving populations of RNA viruses, or even just self-replicating RNA molecules, is not going to be easy. As the persistence of a consensus sequence has been ruled out as a diagnostic, we have to look for markers that are both unambiguous and easy to obtain. Selection for robustness may eventually be observed in natural populations of adapting RNA viruses or viroids, but up to now, no such signals have been reported. While our results show quasispecies effects and the selection for mutational robustness occur regularly in small simulated populations, experimental evidence for these effects remain elusive in real RNA systems. We hope that our demonstration of the frequency and importance of these effects together with the diagnostic markers used to detect them in simulation will help guide future experimental research in this area.

## Acknowledgments

This work was supported in part by NIH Grant AI 065960.

## Appendix A

### A.1. The distribution of the population's average fitness as a random variable

In equilibrium, the distribution of the population's average fitness follows from Wright–Fisher sampling. Define  $\pi$  as the probability that a sequence's offspring will be viable. Without resorting to an explicit form for  $\pi$ , equilibrium and a uniform mutation rate imply that all sequences reproduce successfully with the same probability  $\pi$  (which is in general a function of the mutation rate and the mean neutrality of the population). Denote further the expected value of a random variable  $x$  as  $E[x]$  and its variance as  $V[x]$ . If we take fitness  $w_i$  of the  $i$ th offspring in our population as a random variable, the neutral-network fitness landscape implies that  $w_i$  takes only values 0 or 1, where  $w_i = 1$  occurs with probability  $\pi$ . The distribution of  $w_i$  is therefore a Bernoulli distribution with probability of success  $\pi$ , and we have  $E[w_i] = \pi$  and  $V[w_i] = \pi(1 - \pi)$ .

We now consider the average fitness of the population in equilibrium,  $\langle w \rangle$ , defined as  $\langle w \rangle = (1/N) \sum_{i=1}^N w_i$ . By the central limit theorem, the distribution of  $\langle w \rangle$  will approach a normal distribution  $N[\mu, \sigma^2]$  as  $N \rightarrow \infty$ , and this limit will be reached well before  $N = 1000$  (typically  $N\pi, N(1 - \pi) > 5$  is sufficient (Rice, 1994), and this condition is easily satisfied under all conditions studied). Thus,  $\langle w \rangle$  follows a normal distribution with mean  $\mu = E[w] = \pi$  and variance  $\sigma^2 = V[w] = \pi(1 - \pi)/N$ .

To confirm these assumptions hold, we computed the fitness autocorrelation function within a period of equilibrium. Fig. 8 shows the autocorrelation function for the first equilibrium period shown in Fig. 1 ( $t = 200$ –9814). The autocorrelation drops almost immediately to a mean of nearly zero, and has a noise level  $\sigma \approx 1\%$  to  $2\%$ , consistent with the variation of  $w$  over the time period in question. Similar results hold for each period of fitness equilibrium shown in Fig. 1. In contrast, the population's average neutrality showed significant autocorrelations. While we included the neutrality transitions in Fig. 1 for illustrative purposes, this lack of independence suggests that not all the neutrality steps identified are statistically significant.

### A.2. Identifying jumps in average fitness

Motivated by our observations, we seek to characterize the rapid transitions of the population from lower to higher neutrality states. We derive a statistical test for identifying such transitions a priori in time series data, and associating



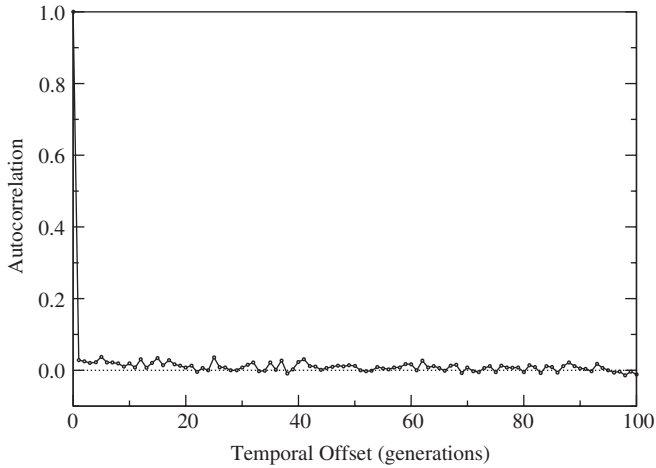


Fig. 8. Temporal autocorrelation function for the first equilibrium period shown in Fig. 1 ( $t = 200-9814$ ).

a  $p$ -value to measure the confidence level of such a transition occurring by chance.

Consider a time series  $w(t) \sim N[\mu, \sigma^2]$  measured at  $T$  sequential points in time. To test the hypothesis of equal means between two specified time periods  $[1, n]$  and  $[n + 1, T]$  is straightforward, and we will assume equal variances for simplicity. We consider the average value of  $w$  over the two periods separately, and consider the sample means  $Y_i$  over the two different time periods, defined by  $Y_1 = (1/n) \sum_{t=1}^n w(t)$  and  $Y_2 = (1/(T - n)) \sum_{t=n+1}^T w(t)$ . These sample means will be normally distributed,  $Y_1 \sim N[\mu, \sigma^2/n]$  and  $Y_2 \sim N[\mu, \sigma^2/(T - n)]$ . Our null hypothesis is that the means will be equal between the two periods. To test this null hypothesis, we consider the difference between the sample means  $D = Y_2 - Y_1$ , and ask whether the observed difference can be explained merely by chance, that is, whether the distribution of  $D$  is consistent with  $D \sim N[0, \sigma_D^2]$ . Here,  $\sigma_D^2$  is the sum of the variances of  $Y_1$  and  $Y_2$ , that is,  $\sigma_D^2 = \sigma^2 T / [n(T - n)]$ .

Thus, under the null hypothesis, the difference of observed means  $D$  is normal with zero mean and known variance, and the associated  $p$ -value can be obtained by looking up the probability of  $Z = D/\sigma_D$  exceeding its observed value in a cumulative distribution table.

We now consider the case of finding the most significant breakpoint in the time series  $[1, T]$  when the division into two periods is unspecified. Letting  $n$  parameterize the number of data points in the first interval, we can consider the above analysis as a function of  $n$ . The highest significance is attained by choosing the maximum value of  $D(n)/\sigma_D(n)$ , where the difference of means and its variance must be calculated for all  $n$  in  $[1, T - 1]$ . Let  $p_n$  represent the  $p$ -value associated with this maximum  $n$ . We wish to know the probability that this maximum level of significance will occur merely by chance due to the fluctuations in  $w(t)$ . Given  $T - 1$  independent trials with probability  $p_n$  of exceeding our maximum level of significance, we see that the probability of all of these trials

resulting in a smaller significance than that of  $p_n$  is

$$\begin{aligned} \Pr[\text{all } T - 1 \text{ of the } p_i \text{ satisfy } p_i < p_n] \\ &= (1 - p_n)^{T-1} \\ &\approx 1 - (T - 1)p_n \quad \text{for } p_n \ll 1. \end{aligned} \tag{A.1}$$

From this probability, we calculate the  $p$ -value associated with any  $p_i$  exceeding our  $p_n$  by chance alone, using the above probability:

$$\begin{aligned} p &= \Pr[\text{at least one } p_i \text{ has } p_i > p_n] \\ &= 1 - \Pr[\text{all } T - 1 \text{ of the } p_i \text{ satisfy } p_i < p_n] \\ &= 1 - (1 - p_n)^{T-1} \approx (T - 1)p_n. \end{aligned} \tag{A.2}$$

Note that the  $T - 1$  other choices of breakpoints are by no means independent of each other, as they all refer to the same underlying fitness data,  $w(t)$ . These correlations reduce the number of effective degrees of freedom, and hence the  $T - 1$  factor will be a conservative overestimate of the actual  $p$ -value. If multiple transitions are expected, this algorithm can be repeated on each subinterval to determine whether further breakpoints are consistent with the given level of statistical confidence.

## References

- Bloom, J.D., Silberg, J.J., Wilke, C.O., Drummond, D.A., Adami, C., Arnold, F.H., 2005. Thermodynamic prediction of protein neutrality. *Proc. Natl Acad. Sci. USA* 102, 606–611.
- Bornberg-Bauer, E., Chan, H.S., 1999. Modeling evolutionary landscapes: mutational stability, topology, and superfunnels in sequence space. *Proc. Natl Acad. Sci. USA* 96, 10689–10694.
- Burch, C.L., Chao, L., 2000. Evolvability of an RNA virus is determined by its mutational neighbourhood. *Nature* 406, 625–628.
- Cowperthwaite, M.C., Bull, J.J., Meyers, L.A., 2005. Distributions of beneficial fitness effects in RNA. *Genetics* 70, 1449–1457.
- Demetrius, L., Schuster, P., Sigmund, K., 1985. Polynucleotide evolution and branching processes. *Bull. Math. Biol.* 47, 239–262.
- Derrida, B., Peliti, L., 1991. Evolution in a flat fitness landscape. *Bull. Math. Biol.* 53, 355–382.
- Domingo, E., 1992. Genetic variation and quasispecies. *Curr. Opin. Genet. Dev.* 288, 61–63.
- Domingo, E., 2002. Quasispecies theory in virology. *J. Virol.* 76, 463–465.
- Domingo, E., Holland, J.J., 1997. RNA virus mutations and fitness for survival. *Annu. Rev. Microbiol.* 51, 151–178.
- Domingo, E., Sabo, D., Taniguchi, T., Weissmann, C., 1978. Nucleotide sequence heterogeneity of an RNA phage population. *Cell* 13, 735–744.
- Domingo, E., Biebricher, C.K., Eigen, M., Holland, J.J., 2001. Quasispecies and RNA Virus Evolution: Principles and Consequences. Landes Bioscience, Georgetown, TX.
- Drake, J.W., 1993. Rates of spontaneous mutation among RNA viruses. *Proc. Natl Acad. Sci. USA* 90, 4171–4175.
- Drake, J.W., Holland, J.J., 1999. Mutation rates among RNA viruses. *Proc. Natl Acad. Sci. USA* 96, 13910–13913.
- Eigen, M., 1971. Selforganization of matter and the evolution of macromolecules. *Die Naturwiss.* 58, 465–523.
- Eigen, M., 1996. On the nature of virus quasispecies. *Trends Microbiol.* 4, 216–218.
- Eigen, M., Schuster, P., 1979. The Hypercycle—A Principle of Natural Self-Organization. Springer, Berlin.
- Fontana, W., Schuster, P., 1998a. Continuity in evolution: On the nature of transitions. *Science* 280, 1451–1455.

- Fontana, W., Schuster, P., 1998b. Shaping space: The possible and the attainable in RNA genotype-phenotype mapping. *J. Theor. Biol.* 194, 491–515.
- Fontana, W., Stadler, P.F., Bornberg-Bauer, E.G., Griesmacher, T., Hofacker, I.L., Tacker, M., Tarazona, P., Weinberger, E.D., Schuster, P., 1993. RNA folding and combinatorial landscapes. *Phys. Rev. E* 47, 2083–2099.
- Forst, C.V., Reidys, C., Weber, J., 1995. Evolutionary dynamics and optimization: Neutral networks as model-landscape for RNA secondary-structure folding-landscapes. In: Morán, F., Moreno, A., Merelo, J.J., Chacón, P. (Eds.), *Advances in Artificial Life, Lecture Notes in Artificial Intelligence*, vol. 929, Springer, Berlin, pp. 128–147.
- Grüner, W., Giegerich, R., Strothmann, D., Reidys, C., Weber, J., Hofacker, I.L., Stadler, P.F., Schuster, P., 1996a. Analysis of RNA sequence structure maps by exhaustive enumeration. 1. Neutral networks. *Monatsh. Chem.* 127, 355–374.
- Grüner, W., Giegerich, R., Strothmann, D., Reidys, C., Weber, J., Hofacker, I.L., Stadler, P.F., Schuster, P., 1996b. Analysis of RNA sequence structure maps by exhaustive enumeration. 2. Structures of neutral networks and shape space covering. *Monatsh. Chem.* 127, 375–389.
- Higgs, P.G., Derrida, B., 1991. Stochastic models for species formation in evolving populations. *J. Phys. A (Math. & Gen.)* 24, L985–L991.
- Higgs, P.G., Derrida, B., 1992. Genetic distance and species formation in evolving populations. *J. Mol. Evol.* 35, 454–465.
- Hofacker, I.L., Fontana, W., Stadler, P.F., Bonhoeffer, S., Tacker, M., Schuster, P., 1994. Fast folding and comparison of RNA secondary structures. *Monatsh. Chem.* 125, 167–188.
- Holmes, E.C., Moya, A., 2002. Is the quasispecies concept relevant to RNA viruses? *J. Virol.* 76, 460–462.
- Hutton, R.J., Broadbent, P., Bevington, K.B., 2000. Viroid dwarfing for high density citrus plantings. *Hortic. Rev.* 24, 277–317.
- Huynen, M.A., 1996. Exploring phenotype space through neutral evolution. *J. Mol. Evol.* 43, 165–169.
- Huynen, M.A., Hogeweg, P., 1994. Pattern generation in molecular evolution: Exploitation of the variation in RNA landscapes. *J. Mol. Evol.* 39, 71–79.
- Huynen, M.A., Stadler, P.F., Fontana, W., 1996. Smoothness within ruggedness: The role of neutrality in adaptation. *Proc. Natl Acad. Sci. USA* 93, 397–401.
- Jenkins, G.M., Worobey, M., Woelk, C.H., Holmes, E.C., 2001. Evidence for the non-quasispecies evolution of RNA viruses. *Mol. Biol. Evol.* 18, 987–994.
- Keese, P., Symons, R., 1985. Domains in viroids: Evidence of intermolecular RNA rearrangements and their contribution to viroid evolution. *Proc. Natl Acad. Sci. USA* 82, 4582–4586.
- Kimura, M., 1962. On the probability of fixation of mutant genes in a population. *Genetics* 47, 713–719.
- Meyers, L.A., Lee, J.F., Cowperthwaite, M., Ellington, A.D., 2004. The robustness of naturally and artificially selected nucleic acid secondary structures. *J. Mol. Evol.* 58, 681–691.
- Novella, I.S., 2004. Negative effect of genetic bottlenecks on the adaptability of vesicular stomatitis virus. *J. Mol. Biol.* 336, 61–67.
- Nowak, M.A., Schuster, P., 1989. Error thresholds of replication in finite populations—Mutation frequencies and the onset of muller's ratchet. *J. Theor. Biol.* 137, 375–395.
- Owens, R.A., Thompson, S.M., 2005. Mutational analysis does not support the existence of a putative tertiary structural element in the left terminal domain of *Potato spindle tuber viroid*. *J. Gen. Virol.* 86, 1835–1839.
- Reidys, C., Stadler, P., Schuster, P., 1997. Generic properties of combinatorial maps: Neutral networks on RNA secondary structures. *Bull. Math. Biol.* 59, 339–397.
- Reidys, C., Forst, C.V., Schuster, P., 2001. Replication and mutation on neutral networks. *Bull. Math. Biol.* 63, 57–94.
- Rice, J.A., 1994. *Mathematical Statistics and Data Analysis*, second ed. Duxbury Press.
- Schuster, P., Swetina, J., 1988. Stationary mutant distributions and evolutionary optimization. *Bull. Math. Biol.* 50, 635–660.
- Schuster, P., Fontana, W., Stadler, P.F., Hofacker, I.L., 1994. From sequences to shapes and back: A case study in rna secondary structures. *Proc. R. Soc. London (Biol)* 255, 279–284.
- Steinhauer, D.A., de la Torre, J.C., Meier, E., Holland, J.J., 1989. Extreme heterogeneity in populations of vesicular stomatitis virus. *J. Virol.* 63, 2072–2080.
- van Lint, J.H., Wilson, R.M., 2001. *A Course in Combinatorics*, second ed. Cambridge University Press, Cambridge.
- van Nimwegen, E., Crutchfield, J.P., Huynen, M., 1999. Neutral evolution of mutational robustness. *Proc. Natl Acad. Sci. USA* 96, 9716–9720.
- Walter, A.E., Turner, D.H., Kim, J., Lyttle, M.H., Müller, P., Mathews, D.H., Zuker, M., 1994. Coaxial stacking of helices enhances binding of oligoribonucleotides and improves predictions of RNA folding. *Proc. Natl Acad. Sci. USA* 91, 9218–9222.
- Wilke, C.O., 2001a. Adaptive evolution on neutral networks. *Bull. Math. Biol.* 63, 715–730.
- Wilke, C.O., 2001b. Selection for fitness versus selection for robustness in RNA secondary structure folding. *Evolution* 55, 2412–2420.
- Wilke, C.O., 2004. Molecular clock in neutral protein evolution. *BMC Genetics* 5, 25.
- Wilke, C.O., Adami, C., 2001. Interaction between directional epistasis and average mutational effects. *Proc. R. Soc. London Ser. B* 268, 1469.
- Wilke, C.O., Adami, C., 2003. Evolution of mutational robustness. *Mutat. Res.* 522, 3–11.
- Wilke, C.O., Wang, J.L., Ofria, C., Lenski, R.E., Adami, C., 2001. Evolution of digital organisms at high mutation rate leads to survival of the flattest. *Nature* 412, 331–333.
- Wilke, C.O., Lenski, R.E., Adami, C., 2003. Compensatory mutations cause excess of antagonistic epistasis in RNA secondary structure folding. *BMC Evol. Biol.* 3, 3.
- Wolf, J.B., Brodie, E.D., Wade, M.J., 2000. *Epistasis and the Evolutionary Process*. Oxford University Press, Oxford.

## Further reading

- Wagner, G.P., Krall, P., 1993. What is the difference between models of error thresholds and Muller's ratchet? *J. Math. Biol.* 32, 33–44.
- Wiehe, T., 1997. Model dependency of error thresholds: The role of fitness functions and contrasts between the finite and infinite sites models. *Genet. Res.* 69, 127–136.
- Wilke, C.O., 2005. Quasispecies theory in the context of population genetics. *BMC Evol. Biol.* 5, 44.